

19 **ABSTRACT**

20 The cell nuclei of Ophisthokonts, the eukaryotic supergroup defined by fungi and
21 metazoans, is remarkable in the constancy of both their double-membraned structure and
22 protein composition. Such remarkable structural conservation underscores common and
23 ancient evolutionary origins. Yet, the dynamics of disassembly and reassembly displayed
24 by Ophisthokont nuclei vary extensively. Besides closed mitosis in fungi and open mitosis
25 in some animals, little is known about the evolution of nuclear envelope break down
26 (NEBD) during cell division. Here, we uncovered a novel form of NEBD in primary
27 oocytes of the flatworm *Schmidtea mediterranea*. From zygotene to metaphase II, both
28 nuclear envelope (NE) and peripheral endoplasmic reticulum (ER) expand notably in size,
29 likely involving *de novo* membrane synthesis. 3-D electron microscopy reconstructions
30 demonstrated that the NE transforms itself into numerous double-membraned vesicles
31 similar in membrane architecture to NE doublets in mammalian oocytes after germinal
32 vesicle breakdown. The vesicles are devoid of nuclear pore complexes and DNA, yet are
33 loaded with nuclear proteins, including a planarian homologue of PIWI, a protein essential
34 for the maintenance of stem cells in this and other organisms. Our data contribute a new
35 model to the canonical view of NE dynamics and support that NEBD is an evolutionarily
36 adaptable trait in multicellular organisms.

37

38 **INTRODUCTION**

39 Nuclear envelope (NE), which is the boundary of the nucleus, is a defining feature
40 of all eukaryotes. NE serves as a barrier for cytoplasmic and nuclear contents and activity,
41 i.e., protein translation, mRNA transcription and DNA replication. Yet, it also poses a
42 challenge to eukaryotic cell divisions: to separate linear chromosomes enclosed by the NE
43 through assembly/disassembly of microtubules located in the cytoplasm.

44 Nature has evolved diverse solutions in Ophisthokonts to tackle this challenge of
45 cell division [1-8]. Such solutions involve multiple modes of NE remodeling to allow
46 accessibility to chromosomes by microtubules. The most straight-forward solution is open
47 mitosis. As NE ruptures into pieces, chromosomes are completely exposed to cytoplasmic
48 microtubules and establish contact through kinetochores. Cases were found, mostly in

49 unicellular organisms, that complete rupture of NE is not necessary. In semi-open mitosis,
50 small holes open locally on NE for adjacent microtubules to access condensed
51 chromosomes within the nuclei. In closed mitosis, microtubule organization center
52 (MTOC), is embedded in the NE during all or part of the cell cycle.

53 Among all the diverse modes of NE regulation during cell divisions, whether
54 vesiculation is a disfavored strategy by natural selection remains controversial [9, 10]. The
55 fate of NE proteins after NE breakdown and the source of NE proteins for the assembly of
56 new NE in daughter cells underlies the motivation of a proposed vesiculation model four
57 decades ago [11, 12]. In this model, the nucleus breaks down into multiple vesicles with
58 pieces of NE enclosing portions of the nuclear content, while chromosomes are exposed to
59 cytoplasmic factors. Accumulating evidence supports an otherwise mutually exclusive
60 model, that NE proteins are dispersed into the peripheral ER upon NEBD and comes from
61 the ER network upon assembly of a new nucleus, and challenges the experimental methods
62 in earlier studies. While in principle, NE vesiculation maintains barrier function between
63 cytoplasm and nucleus materials, as is in closed mitosis, and allows for full accessibility to
64 the condensed chromosomes by microtubules, as is in open mitosis, whether this solution
65 for cell division indeed exists in nature needs direct evidence.

66

67 **RESULTS AND DISCUSSION**

68 **Meiotic progression can be detected and stages quantified in planarian ovaries.**

69 Here, we examined NEBD during oocyte meiosis in a free-living fresh water
70 flatworm, *Schmidtea mediterranea*, which has been established as a model system to study
71 adult stem cells, regeneration, and germ cell specification [13-22]. Detected widespread
72 maintenance of genome heterozygosity suggests potential mechanisms in meiosis [23, 24].
73 Yet, meiosis has only been studied in the testis [25].

74 To characterize female meiosis in *S. mediterranea*, we examined the ovaries using
75 Transmission Electron Microscopy (TEM). Ultrastructural studies revealed five categories
76 of cells with oocyte features (Figure 1; Supplementary Fig.1). These cells are in close
77 proximity to each other in a relatively compacted area of the ovary (Figure 1A), are of
78 much larger size (20~50 μ m in diameter) than most somatic cells (10~20 μ m), and contain

79 germ cell specific organelles (*e.g.*, chromatoid body [26-35] and annulate lamella [36-43]
80) (Supplementary Fig.1). We grouped cells into five categories based on their nuclear
81 morphology. Type-I cells have smaller nuclei with multiple Synaptonemal Complexes
82 (SYCPs) [44-47] (Figure 1B, Supplementary Fig.2), suggesting they are oocytes at
83 zygotene or pachytene stage of prophase I. Type-II cells have undulating NEs, and
84 remnants of SYCPs, characterized by high electron density, short dark stripes (Figure 1B).
85 The dissolution of SYCP suggests Type-II cells are entering diplotene stage of prophase I.
86 Type-III, IV and V cells have numerous vesicular structures surrounding the NE and dense
87 patches of condensed chromatins inside the NE (Figure 1C-E). In Type-IV cells, vesicles
88 are elongated. In Type-V cells, the vesicles are in the cytoplasmic periphery, and shaped
89 like dumbbells.

90 As free ribosomes are easily recognizable and almost evenly distributed in the
91 cytoplasm of all cells, we quantified densities of free ribosomes to examine relationships
92 of these cells. From Type-I to Type-V cells, a gradual decrease in free ribosome density
93 was observed, suggesting Type-I to Type-V cells are oocytes at progressive steps of
94 meiosis (Figure 1F). Consistently, distances of the proximal ends of the vesicles to the NE
95 steadily increase from Type-III to Type-V cells (Figure 1G), which are diplotene to
96 diakinesis stages of prophase I. As ovulated oocytes are arrested at metaphase II [23],
97 meiosis stages from prophase I to metaphase II likely take place as the oocytes travel
98 through the tuba and oviduct to the female atrium [48]. Alternatively, missing steps in
99 meiosis could be fast and transient, which would be difficult to detect in the ovary.

100 **Nuclear envelope breakdown of planarian oocytes yields abundant, double-** 101 **membraned vesicles.**

102 Five features define the perinuclear vesicles as novel NE-associated subcellular
103 organelles. First, they are double membraned and distinct from peripheral ER (Figure1H).
104 Second, ribosomes decorate the outer membrane of the vesicles (Figure1H,I). Third,
105 electron density in the interior of the vesicles are comparable to nucleoplasm, but distinct
106 from cytoplasm (Figure1H,J,K). Fourth, distances between the inner and outer membranes
107 are comparable to the NE (Figure1H,J,K). Fifth, membranes of some vesicles can be
108 physically continuous with the NE but lacking nuclear pore complexes (NPCs) (Figure 1J).

109 Interestingly, NPCs are present in the NE immediately adjacent to the emerging vesicles.
110 Specific regulations of NPCs on the vesicles are likely due to three mechanisms: vesicles
111 form with newly synthesized NE without NPCs; vesicles form with pre-existing NE on
112 which NPCs are selectively disassembled; NPCs are disassembled and dispersed on the
113 vesicle membranes.

114 While in Type-III cells the vesicles are dumpy and adjacent to the NE (Figure 1K),
115 they are dumbbell shaped and far away from the NE in Type-V cells (Figure 1L). Hence,
116 the formation of perinuclear vesicles is very dynamic. As it appears that these vesicles
117 radiate from NE (Figure 1C-E), we named them Sunburst NE Vesicles (SNEVs).

118 **Nuclear membrane vesiculation products are topologically complex.**

119 To clarify the dynamics of SNEV formation, we reconstructed 3-D models from
120 serial sections of the oocytes. SNEVs start as double-membraned buds of NE in Type-III
121 cells (Figure2A). The buds grow distally, branch out and fold onto themselves (Figure2B,).
122 In Type-V cells, the SNEVs are elongated, with the proximal ends arranged as tubules and
123 the distal ends as flattened, stacked sheets (Figure2C-E). Some SNEVs appear
124 disconnected from the NE (Figure2C,F-I).

125 3-D models revealed topological complexity of the SNEVs in Type-V cells. SNEVs
126 are dumbbell-shaped in some sections, but appear with variable shapes (*e.g.*, rings) in other
127 sections (Figure2D-I). The encapsulated space of the vesicles is not spherical. Instead,
128 some areas of the inner vesicle membranes are in close proximity.

129 To examine the fate of the SNEVs after oocyte maturation, ovulated oocytes in egg
130 capsules, which are arrested at metaphase II [23], were studied. In general, cytoplasmic
131 space of ovulated oocytes is filled in its entirety with membrane units of variable sizes and
132 shapes (Figure3A-B). Nonetheless, all membrane units are topologically similarly
133 organized (Figure 3B). Switching from short and oval shapes of the SNEVs in Type-III
134 oocytes to dumbbell shapes in Type-V oocytes implicates a tendency of double-layered
135 membranes to form four-layered doublets (Figure 3C, left to right). The membrane units in
136 metaphase II oocytes have long stretches of such four-layered doublets (Figure3D). In fact,
137 these four-layered doublets are very prominent and comparable to NE doublets in mice and
138 human oocytes after germinal vesicle breakdown (GVBD) [49-51] (Supplementary Figure

139 3D). In both cases, the inner membranes of the two double layered membranes are the
140 contacting surfaces. Doublet formation could be a general property of membranes in the
141 oocytes.

142 Taken together, the dynamics of SNEVs and the disappearance of nuclei in
143 metaphase II oocytes define a novel form of NEBD or GVBD.

144 **Double-membraned vesicles are filled with nucleoplasmic proteins**

145 To examine the fate of nuclear proteins during NEBD, antibodies against the
146 Argonaute protein family PIWI protein SMEDWI-2 [52-56] and Histone H3 were used to
147 characterize the dynamics of SNEV formation. Immunohistological studies revealed
148 SMEDWI-2 persists in the nucleus during all stages of prophase I, where it marks SNEV-
149 like structures (Figure4A-C). This is contrast to cytoplasmic SMEDWI-1 protein, which is
150 degraded as the oocyte matures (Supplementary Figure 3A). Histone H3 protein shows the
151 same dynamics in the nucleus and in SNEVs as SMEDWI-2 (Supplementary Figures 3B-
152 C). These data conclude nuclear proteins are packaged into SNEVs. Interestingly,
153 chromosomes are specifically excluded since these vesicles are negative for DNA dyes
154 (*e.g.*, DAPI, Hoechst 33342) (Figure 4, Supplementary Figures 3B-C).

155 Metaphase II stage oocytes with four condensed chromosomes can be found in the
156 ovary at low frequency. The distribution of SMEDWI-2 protein in metaphase II stage
157 oocytes (Figure 4D) in the ovary is consistent with our ultrastructural findings in the
158 ovulated oocytes. There, the nucleus is dissolved into individual SNEV units of variable
159 size and morphology (Figure 3), supporting the view that SNEV formation involves mass
160 encapsulation of nuclear contents as vesicles dispersed throughout the cytoplasm.

161 **Marked expansion of nuclear double-layered membranes occurs during planarian** 162 **oocyte NE breakdown**

163 The formation of SNEVs is accompanied by an expansion of NE surface area. As
164 oocytes mature, cell volume increases approximately 8 times from pachytene to diplotene
165 stages (Figure4A,C; Figure5A-B; Supplementary Figure3B-C). To maintain a constant
166 nuclear to cytoplasmic ratio [57-59], nuclear volume thus increases, leading to a 4-fold
167 expansion of the NE surface area in case of a spherical nucleus. In addition, partitioning

168 nuclear volume into much smaller vesicles leads to a significant increase in surface area.
169 The larger the number of SNEVs, the more the membrane surface area increases. We
170 estimated a 40-fold expansion of nuclear double-layered membranes in total (Methods).

171 **ER is unlikely to serve as a membrane reservoir for double-membraned vesicle** 172 **biogenesis**

173 To examine whether expansion of NE/SNEV surface area leads to a net decrease
174 of peripheral ER, a SEC61A [60-64] antibody was used to visualize the ER network. The
175 distinctive staining patterns of SEC61A and Histone H3 (Figure5A-B) suggest that
176 SEC61A is mostly localized on the peripheral ER instead of the NE. Line profiling showed
177 that SEC61A can co-localize with Histone H3 (Figure5B-C). However, even in such areas,
178 most of the SEC61A signal is separated from Histone H3 signal in "salt and pepper"
179 patterns (Figures5B-C). The independent organization and occasional physical interaction
180 of peripheral ER and elongating SNEVs were verified by TEM (Figures5D-E). Direct
181 interaction between tubular ER and elongating SNEVs suggests tubular ER may contribute
182 to the elongation process. One possible function is to provide membranes. However, no
183 clear reduction of the peripheral ER network is observed (Figures5A-B). Collectively, the
184 ER-NE-SNEV membrane system expands in size as the oocytes mature. Hence, *de novo*
185 membrane synthesis is likely required for the formation of SNEVs.

186 **Conclusions**

187 Our data provided direct evidence that nuclear envelope can break down into
188 vesicles during cell division, highlighting a new paradigm of nuclei dynamics in
189 Ophisthokont. NE vesiculation is likely a trait adapted to the biology of the superphylum
190 Platyhelminths. Establishment of double-membraned vesicles from NE were noted in
191 female gonads in three other species from Platyhelminths, *Cura foremanii*, *Sabussowia*
192 *dioica*, and *Vorticeros luteum* [65-67]. Confusion of these double-membraned vesicles
193 with peripheral ER [68] only emphasizes that NE vesiculation has not been recognized.

194 What are the functions of SNEVs? Requirement of *de novo* membrane synthesis
195 and specific regulation of NPCs support that SNEVs are not units for waste disposal but
196 instead tightly regulated structures. As NE vesiculation was found specific to female
197 meiosis, we speculate that SNEV formation is a strategy to regulate the fate of nucleoplasm

198 after GVBD and the establishment of pluripotency in the zygote. While SMEDWI-1 is
199 degraded during oocyte maturation (Supplementary Figure 3A), nuclear SMEDWI-2 is
200 preserved. Importantly, loss of SMEDWI-1 does not show a phenotype in adult planarians,
201 whereas abrogation of SMEDWI-2 leads to loss of somatic stem cells and death of the
202 worms [53, 69-71]. Additionally, SNEVs may direct nucleoplasm to chromosomes for
203 reassembly of the zygote nucleus, and jump-start mitotic divisions in early embryonic
204 development.

205 References

- 206
- 207 1. Heath, I.B., *Variant Mitoses in Lower Eukaryotes: Indicators of the Evolution of*
208 *Mitosis?*, in *International Review of Cytology*, J.F.D. G.H. Bourne and K.W.
209 Jeon, Editors. 1980, Academic Press. p. 1-80.
- 210 2. Kutay, U. and M.W. Hetzer, *Reorganization of the Nuclear Envelope during*
211 *Open Mitosis*. *Current opinion in cell biology*, 2008. **20**(6): p. 669-677.
- 212 3. Guttinger, S., E. Laurell, and U. Kutay, *Orchestrating nuclear envelope*
213 *disassembly and reassembly during mitosis*. *Nat Rev Mol Cell Biol*, 2009. **10**(3):
214 p. 178-191.
- 215 4. De Souza, C.P.C. and S.A. Osmani, *Mitosis, Not Just Open or Closed*. *Eukaryotic*
216 *Cell*, 2007. **6**(9): p. 1521-1527.
- 217 5. Anderson, D.J. and M.W. Hetzer, *The life cycle of the metazoan nuclear envelope*.
218 *Current opinion in cell biology*, 2008. **20**(4): p. 386-392.
- 219 6. Drechsler, H. and A.D. McAinsh, *Exotic mitotic mechanisms*. *Open Biology*,
220 2012. **2**(12): p. 120140.
- 221 7. Arnone, J.T., A.D. Walters, and O. Cohen-Fix, *The dynamic nature of the nuclear*
222 *envelope: lessons from closed mitosis*. *Nucleus*, 2013. **4**(4): p. 261-6.
- 223 8. Smoyer, C.J. and S.L. Jaspersen, *Breaking down the wall: the nuclear envelope*
224 *during mitosis*. *Curr Opin Cell Biol*, 2014. **26**: p. 1-9.
- 225 9. Burke, B. and J. Ellenberg, *Remodelling the walls of the nucleus*. *Nat Rev Mol*
226 *Cell Biol*, 2002. **3**(7): p. 487-497.
- 227 10. Collas, P. and J.-C. Courvalin, *Sorting nuclear membrane proteins at mitosis*.
228 *Trends in Cell Biology*, 2000. **10**(1): p. 5-8.
- 229 11. Lohka, M.J. and Y. Masui, *Formation in vitro of sperm pronuclei and mitotic*
230 *chromosomes induced by amphibian ooplasmic components*. *Science*, 1983.
231 **220**(4598): p. 719-721.
- 232 12. Zeligs, J.D. and S.H. Wollman, *Mitosis in rat thyroid epithelial cells in vivo. I.*
233 *Ultrastructural changes in cytoplasmic organelles during the mitotic cycle*. *J*
234 *Ultrastruct Res*, 1979. **66**(1): p. 53-77.
- 235 13. Sanchez Alvarado, A. and P.A. Tsonis, *Bridging the regeneration gap: genetic*
236 *insights from diverse animal models*. *Nat Rev Genet*, 2006. **7**(11): p. 873-84.
- 237 14. King, R.S. and P.A. Newmark, *The cell biology of regeneration*. *J Cell Biol*,
238 2012. **196**(5): p. 553-62.

- 239 15. Pellettieri, J. and A. Sanchez Alvarado, *Cell turnover and adult tissue*
240 *homeostasis: from humans to planarians*. *Annu Rev Genet*, 2007. **41**: p. 83-105.
- 241 16. Reddien, P.W., *The Cellular and Molecular Basis for Planarian Regeneration*.
242 *Cell*, 2018. **175**(2): p. 327-345.
- 243 17. Wang, Y., et al., *A functional genomic screen in planarians identifies novel*
244 *regulators of germ cell development*. *Genes Dev*, 2010. **24**(18): p. 2081-92.
- 245 18. Chong, T., et al., *Molecular markers to characterize the hermaphroditic*
246 *reproductive system of the planarian Schmidtea mediterranea*. *BMC Dev Biol*,
247 2011. **11**: p. 69.
- 248 19. Zayas, R.M., et al., *The planarian Schmidtea mediterranea as a model for*
249 *epigenetic germ cell specification: analysis of ESTs from the hermaphroditic*
250 *strain*. *Proc Natl Acad Sci U S A*, 2005. **102**(51): p. 18491-6.
- 251 20. Agata, K., *Regeneration and gene regulation in planarians*. *Curr Opin Genet*
252 *Dev*, 2003. **13**(5): p. 492-6.
- 253 21. Rink, J.C., *Stem cell systems and regeneration in planaria*. *Development Genes*
254 *and Evolution*, 2013. **223**(1-2): p. 67-84.
- 255 22. Pearson, B.J. and A. Sanchez Alvarado, *Regeneration, stem cells, and the*
256 *evolution of tumor suppression*. *Cold Spring Harb Symp Quant Biol*, 2008. **73**: p.
257 565-72.
- 258 23. Guo, L., et al., *Widespread maintenance of genome heterozygosity in*
259 *Schmidtea mediterranea*. *Nature Ecology & Evolution*, 2016. **1**: p. 0019.
- 260 24. Grohme, M.A., et al., *The genome of Schmidtea mediterranea and the evolution of*
261 *core cellular mechanisms*. *Nature*, 2018. **554**(7690): p. 56-61.
- 262 25. Xiang, Y., et al., *Synaptonemal complex extension from clustered telomeres*
263 *mediates full-length chromosome pairing in Schmidtea mediterranea*. *Proc Natl*
264 *Acad Sci U S A*, 2014. **111**(48): p. E5159-68.
- 265 26. Coward, S.J., *Chromatoid bodies in somatic cells of the planarian: Observations*
266 *on their behavior during mitosis*. *The Anatomical Record*, 1974. **180**(3): p. 533-
267 545.
- 268 27. Kotaja, N. and P. Sassone-Corsi, *The chromatoid body: a germ-cell-specific RNA-*
269 *processing centre*. *Nat Rev Mol Cell Biol*, 2007. **8**(1): p. 85-90.
- 270 28. Solana, J., P. Lasko, and R. Romero, *Spoltud-1 is a chromatoid body component*
271 *required for planarian long-term stem cell self-renewal*. *Developmental Biology*,
272 2009. **328**(2): p. 410-421.
- 273 29. Rouhana, L., et al., *PRMT5 and the role of symmetrical dimethylarginine in*
274 *chromatoid bodies of planarian stem cells*. *Development*, 2012. **139**(6): p. 1083-
275 1094.
- 276 30. Rouhana, L., et al., *PIWI homologs mediate Histone H4 mRNA localization to*
277 *planarian chromatoid bodies*. *Development*, 2014. **141**(13): p. 2592-601.
- 278 31. Parvinen, M., *The chromatoid body in spermatogenesis*. *International Journal of*
279 *Andrology*, 2005. **28**(4): p. 189-201.
- 280 32. Ikenishi, K., *Germ plasm in Caenorhabditis elegans, Drosophila and Xenopus*.
281 *Development, Growth & Differentiation*, 1998. **40**(1): p. 1-10.
- 282 33. Kloc, M., S. Bilinski, and L.D. Etkin, *The Balbiani Body and Germ Cell*
283 *Determinants: 150 Years Later*, in *Current Topics in Developmental Biology*, P.S.
284 Gerald, Editor. 2004, Academic Press. p. 1-36.

- 285 34. Al-Mukhtar, K.A.K. and A.C. Webb, *An ultrastructural study of primordial germ*
286 *cells, oogonia and early oocytes in Xenopus laevis*. Journal of Embryology and
287 Experimental Morphology, 1971. **26**(2): p. 195-217.
- 288 35. Agata, K. and K. Watanabe, *Molecular and cellular aspects of planarian*
289 *regeneration*. Semin Cell Dev Biol, 1999. **10**(4): p. 377-83.
- 290 36. Kessel, R.G., *Annulate lamellae*. Journal of ultrastructure research, 1968. **10**: p. 1-
291 82.
- 292 37. Kessel, R.G., *Fine structure of annulate lamellae*. The Journal of Cell Biology,
293 1968. **36**(3): p. 658-664.
- 294 38. Kessel, R.G., *Annulate Lamellae: A Last Frontier in Cellular Organelles*, in
295 *International Review of Cytology*, W.J. Kwang and F. Martin, Editors. 1992,
296 Academic Press. p. 43-120.
- 297 39. Braat, A.K., et al., *Characterization of zebrafish primordial germ cells:*
298 *Morphology and early distribution of vasa RNA*. Developmental Dynamics, 1999.
299 **216**(2): p. 153-167.
- 300 40. Merriam, R.W., *The Origin and Fate of Annulate Lamellae in Maturing Sand*
301 *Dollar Eggs*. The Journal of Biophysical and Biochemical Cytology, 1959. **5**(1):
302 p. 117-122.
- 303 41. Kessel, R.G., *The annulate lamellae—From obscurity to spotlight*. Electron
304 Microscopy Reviews, 1989. **2**(2): p. 257-348.
- 305 42. Barton, B.R. and A.T. Hertig, *Ultrastructure of Annulate Lamellae in Primary*
306 *Oocytes of Chimpanzees (Pan troglodytes)*. Biology of Reproduction, 1972. **6**(1):
307 p. 98-108.
- 308 43. Kessel, R.G., *Intranuclear and cytoplasmic annulate lamellae in tunicate oocytes*.
309 The Journal of Cell Biology, 1965. **24**(3): p. 471.
- 310 44. Wettstein, D., S.W. Rasmussen, and P.B. Holm, *The Synaptonemal Complex in*
311 *Genetic Segregation*. Annual Review of Genetics, 1984. **18**(1): p. 331-411.
- 312 45. Heyting, C., *Synaptonemal complexes: structure and function*. Current Opinion in
313 Cell Biology, 1996. **8**(3): p. 389-396.
- 314 46. Page, S.L. and R.S. Hawley, *The genetics and molecular biology of the*
315 *synaptonemal complex*. Annual Review of Cell and Developmental Biology,
316 2004. **20**(1): p. 525-558.
- 317 47. Gillies, C.B., *Synaptonemal Complex and Chromosome Structure*. Annual
318 Review of Genetics, 1975. **9**(1): p. 91-109.
- 319 48. Hyman, L.H., *The invertebrates: Platyhelminthes and Rhynchocoela* Vol. II.
320 1951: McGraw-Hill Book Company, Inc. . 550.
- 321 49. Calarco, P.G., R.P. Donahue, and D. Szollosi, *Germinal Vesicle Breakdown in the*
322 *Mouse Oocyte*. Journal of Cell Science, 1972. **10**(2): p. 369-385.
- 323 50. Szollosi, D., P.G. Calarco, and R.P. Donahue, *The nuclear envelope: its*
324 *breakdown and fate in mammalian oogonia and oocytes*. Anat Rec, 1972. **174**(3):
325 p. 325-39.
- 326 51. Thibault, C., D. Szollosi, and M. Gerard, *Mammalian oocyte maturation*. Reprod
327 Nutr Dev, 1987. **27**(5): p. 865-96.
- 328 52. Cox, D.N., et al., *A novel class of evolutionarily conserved genes defined by piwi*
329 *are essential for stem cell self-renewal*. Genes & Development, 1998. **12**(23): p.
330 3715-3727.

- 331 53. Reddien, P.W., et al., *SMEDWI-2 is a PIWI-Like Protein That Regulates*
332 *Planarian Stem Cells*. *Science*, 2005. **310**(5752): p. 1327-1330.
- 333 54. Gonzalez, J., et al., *Piwi Is a Key Regulator of Both Somatic and Germline Stem*
334 *Cells in the Drosophila Testis*. *Cell Reports*, 2015. **12**(1): p. 150-161.
- 335 55. Peng, J.C., et al., *Piwi maintains germline stem cells and oogenesis in Drosophila*
336 *through negative regulation of Polycomb group proteins*. *Nat Genet*, 2016. **48**(3):
337 p. 283-291.
- 338 56. Zeng, A., et al., *Heterochromatin protein 1 promotes self-renewal and triggers*
339 *regenerative proliferation in adult stem cells*. *The Journal of Cell Biology*, 2013.
340 **201**(3): p. 409-425.
- 341 57. Huber, M.D. and L. Gerace, *The size-wise nucleus: nuclear volume control in*
342 *eukaryotes*. *The Journal of Cell Biology*, 2007. **179**(4): p. 583-584.
- 343 58. Walters, A.D., A. Bommakanti, and O. Cohen-Fix, *Shaping the Nucleus: Factors*
344 *and Forces*. *Journal of cellular biochemistry*, 2012. **113**(9): p. 2813-2821.
- 345 59. Webster, M., K.L. Witkin, and O. Cohen-Fix, *Sizing up the nucleus: nuclear*
346 *shape, size and nuclear-envelope assembly*. *Journal of Cell Science*, 2009.
347 **122**(10): p. 1477-1486.
- 348 60. Görlich, D., et al., *A mammalian homolog of SEC61p and SECYp is associated*
349 *with ribosomes and nascent polypeptides during translocation*. *Cell*, 1992. **71**(3):
350 p. 489-503.
- 351 61. Hartmann, E., et al., *Evolutionary conservation of components of the protein*
352 *translocation complex*. *Nature*, 1994. **367**(6464): p. 654-657.
- 353 62. Deshaies, R.J. and R. Schekman, *A yeast mutant defective at an early stage in*
354 *import of secretory protein precursors into the endoplasmic reticulum*. *The*
355 *Journal of Cell Biology*, 1987. **105**(2): p. 633-645.
- 356 63. Simon, S.M. and G. Blobel, *A protein-conducting channel in the endoplasmic*
357 *reticulum*. *Cell*, 1991. **65**(3): p. 371-380.
- 358 64. Shao, S. and R.S. Hegde, *Membrane Protein Insertion at the Endoplasmic*
359 *Reticulum*. *Annual Review of Cell and Developmental Biology*, 2011. **27**(1): p.
360 25-56.
- 361 65. Nigro, M. and V. Gremigni, *Ultrastructural features of oogenesis in a free-living*
362 *marine platyhelminth, Vorticeros Luteum*. *Tissue & Cell*, 1987. **19**(3): p. 377-386.
- 363 66. Tekaya, S., et al., *The ovary of the gonochoristic marine triclad Sabussowia*
364 *dioica: ultrastructural and cytochemical investigations*. *Micron*, 1999. **30**: p. 71-
365 83.
- 366 67. Fischlschweiger, W., *Ultrastructure of the reproductive system of Cura foremanii*
367 *(Platyhelminthes: Tricladida)*. *Transactions of the American Microscopical*
368 *Society*, 1994. **113**(1): p. 1-14.
- 369 68. Harrath, A.H., et al., *An ultrastructural study of oogenesis in the planarian*
370 *Schmidtea mediterranea (Platyhelminthe, Paludicola)*. *Comptes Rendus*
371 *Biologies*, 2011. **334**: p. 516-525.
- 372 69. Palakodeti, D., et al., *The PIWI proteins SMEDWI-2 and SMEDWI-3 are required*
373 *for stem cell function and piRNA expression in planarians*. *RNA*, 2008. **14**(6): p.
374 1174-1186.

- 375 70. Shibata, N., et al., *Inheritance of a Nuclear PIWI from Pluripotent Stem Cells by*
376 *Somatic Descendants Ensures Differentiation by Silencing Transposons in*
377 *Planarian*. *Developmental Cell*, 2016. **37**(3): p. 226-237.
- 378 71. Tharp, Marla E. and A. Bortvin, *DjPiwiB: A Rich Nuclear Inheritance for*
379 *Descendants of Planarian Stem Cells*. *Developmental Cell*, 2016. **37**(3): p. 204-
380 206.
- 381 72. Cebrià, F. and P.A. Newmark, *Planarian homologs of netrin and netrin receptor*
382 *are required for proper regeneration of the central nervous system and the*
383 *maintenance of nervous system architecture*. *Development*, 2005. **132**(16): p.
384 3691-3703.
- 385 73. Oviedo, N.J., et al., *Establishing and Maintaining a Colony of Planarians*. *Cold*
386 *Spring Harbor Protocols*, 2008. **2008**(10): p. pdb.prot5053.
- 387 74. Brubacher, J.L., A.P. Vieira, and P.A. Newmark, *Preparation of the planarian*
388 *Schmidtea mediterranea for high-resolution histology and transmission electron*
389 *microscopy*. *Nat. Protocols*, 2014. **9**(3): p. 661-673.
- 390 75. Higuchi, S., et al., *Characterization and categorization of fluorescence activated*
391 *cell sorted planarian stem cells by ultrastructural analysis*. *Development, Growth*
392 *& Differentiation*, 2007. **49**(7): p. 571-581.
- 393 76. Rink, J.C., H.T.-K. Vu, and A.S. Alvarado, *The maintenance and regeneration of*
394 *the planarian excretory system are regulated by EGFR signaling*. *Development*,
395 2011. **138**(17): p. 3769.
- 396 77. Kremer, J.R., D.N. Mastronarde, and J.R. McIntosh, *Computer Visualization of*
397 *Three-Dimensional Image Data Using IMOD*. *Journal of Structural Biology*,
398 1996. **116**(1): p. 71-76.

400 **Materials and Methods**

401 **Worm care**

402 Planarians were maintained in 1x Milli-Q standard planarian medium at 18°C, with
403 constant once or twice a week feeding of organic liver paste [72, 73]. To study the ovaries,
404 sexually mature worms of 1 to 2cm in length were used. Multiple planarian lines were used
405 for the analysis. Data reported were from line S2-3 and S2F8b [23] of *S. mediterranea*. To
406 obtain ovulated oocytes, worms were maintained in solitude as virgins with twice a week
407 feeding.

408 **Transmission Electron Microscopy**

409 For TEM analysis, dissected ovaries were fixed with 2.5% paraformaldehyde/2%
410 glutaraldehyde/PBS for overnight at 4°C. Then the tissues were processed as described

411 with modifications [74-76]. Briefly, the tissues were washed with 0.1 M sodium cacodylate
412 buffer (pH=6.8), intensified in 2% OsO₄/0.1 M sodium cacodylate buffer (pH=6.8), stained
413 with 2% uranium acetate *en bloc*, dehydrated with a graded ethanol series (30%, 50%,
414 70%, 95%, and two times 100%, 10 min each), equilibrated with two incubations (10 min)
415 in propylene oxide, and incubated in 50% propylene oxide/50% Epon resin (EMS, Fort
416 Washington, PA) mixture overnight. The samples were then infiltrated in 100% Epon resin
417 for 4hr, embedded, and polymerized at 60°C for 24 hrs. After sectioning, the images were
418 acquired on a FEI transmission electron microscope (Tecnai Bio-TWIN 12, FEI). 3D EM
419 models were constructed using the IMOD image-processing package [77]. EM images
420 were converted into stacks as .mrc files and then aligned using MIDAS. Volume
421 segmentation, 3d meshing and surface rendering were done in 3dmod. ImageJ was then
422 used for image format conversion.

423 Taking these two factors into account, we measured total circumference of SNEV
424 membranes and NE membranes in Type-V and Type-I oocytes. Images used for the
425 measurements were from sections of oocytes imaged by TEM. From this crude
426 quantification,

427 **Histological sections**

428 Sexually mature worms were fixed with freshly prepared 4% paraformaldehyde (Electron
429 Microscopy Sciences, Catalog no.: 15710) in PBS for one hour at room temperature with
430 gentle shaking. The anterior fragment of the planarians with the ovaries were obtained for
431 paraffin or cryo sections after washing with 1x PBS for three times. The rinse was 20min
432 each. For paraffin processing, worms are dehydrated through graded ethanol (30%, 50% in
433 PBS) and then stored in 70% ethanol at 4°C for overnight. Paraffin blocks were loaded into

434 a Tissue-Tek VIP processor (Sakura, Netherlands), followed by graded ethanol
435 dehydration (70% for 15 min, 80% for 20min, 95% for 15min and 100% for 20min) and
436 xylene substitute substance clearance (10 min/changes for 3 times). After 4 changes of
437 paraffin infiltration (20 min/change), planarian was embedded for sectioning. Paraffin
438 sections with 8um thickness were cut using a Leica RM2255 microtome (Leica Biosystems
439 Inc. Buffalo Grove, IL) and mounted on Superfrost Plus microscope slides (Fisher
440 Scientific,). For cryo processing, fixed planarian was dehydrated through 30% sucrose and
441 followed by embedding with OCT compound (Tissue-Tek, CA). Cryo sections with 14um
442 thickness were cut using a Leica CM3050S cryostat (Leica Biosystems Inc. Buffalo Grove,
443 IL).

444 **Immunofluorescence staining**

445 Paraffin or cryo sections of planarian fragments containing ovaries were used for
446 immunofluorescence staining. Antibodies anti-SEC61A, anti-Histone H3 and anti-ds DNA
447 was from Abcam (Catalog no.: ab183046, ab1791, ab24834, and ab27156). SEC61A is an
448 evolutionarily conserved subunit of the Sec61/SecY complex, an ER apparatus that
449 translocates nascent membrane proteins into the ER. SMED-SEC61A protein sequence is
450 86% identical to the human SEC61A isoform 1. Anti-SMEDWI1 was a kind gift from Dr.
451 Jochen Rink. Anti-SMEDWI2 was a kind gift from Dr. Claus-D. Kuhn and Dr. Qing Jing.
452 Goat anti-mouse IgG secondary antibody Alexa Fluor 488, and goat anti-rabbit secondary
453 antibody Alexa Fluor 647 were from Thermo Fisher Scientific (Catalog no.: A-11001, and
454 A-21245). Generally, histological sections were rinsed with PBS with 0.5% Triton X-100
455 for three times. The rinse is 10 minutes each. Tissues were digested with 2µg/ml Proteinase
456 K (Thermo Fisher Scientific, 25530049) and 0.1% SDS for 10min at room temperature in

457 PBS with 0.5% Triton X-100. After extensive washes, tissues were incubated with 10%
458 Horse serum (Sigma, H1138) in PBS with 0.5% Triton X-100 for one hour at room
459 temperature. All primary antibodies were used as 1:100 dilution in the blocking solution
460 (10% Horse serum in PBS with 0.5% Triton X-100). Tissues were incubated with primary
461 antibodies overnight at 4°C with gentle shaking. After three washes, the tissues were
462 incubated with secondary antibodies overnight 4°C with gentle shaking. All secondary
463 antibodies were used as 1:300 dilution in the blocking solution. Hoechst 33342 (Thermo
464 Fisher Scientific, H3570) was used as 1:300 to stain the tissues for 30min at room
465 temperature during washes. Slides were mounted with Prolong Diamond Antifade
466 Mountant (Thermo Fisher Scientific, P36965).

467 **Image acquisition**

468 All fluorescence images were acquired with ZEN software. All raw data were saved as
469 16bit images. Zeiss LSM-780 Confocal Microscope and Alpha Plan-Apochromat
470 100x/1.46 Oil DIC objective were used for most images reported. Zeiss LSM-710 Confocal
471 Microscope and Alpha Plan-Apochromat 63x/1.46 Oil Korr M27 objective were used for
472 Supplementary Figure 3A with a zooming factor of 0.7. For double staining with anti-
473 SEC61A and anti-Histone H3 (Figure 5), lasers 633 and 488 were used. Fiji is used for all
474 image processing.

475

476 **Acknowledgements**

477 The authors would like to thank Drs. Jochen Rink and Qing Jing for sharing SMEDWI-1
478 and SMEDWI-2 antibodies. We would like to thank Dr. Elizabeth M. Duncan for
479 suggestions and sharing of histone antibodies, Dr. Sue Jaspersen for revising the

480 manuscript, and suggestions of ER markers, Drs. Christopher P. Arnold and Stephanie
481 Nowotarski for revising the manuscript, Dr. Yongfu Wang for histological sections and
482 antibody testing, Dr. Zulin Yu for assistance in imaging, Mr. Eric Ross for identifying
483 reticulon homologues in *S. mediterranea*, and Mr. Mark Miller for illustration. We would
484 like to thank Dr. Isabel Espinosa Medina for translation of the French article, Jillian
485 Thaden, Katie Evans, Andrew Vogelsang, Corey Abrams, Shane M. Merryman, and Diana
486 Baumann from the Stowers Aquatics Facility for skillful management of the planarians.
487 This work was funded in part by NIH R37GM057260 to A.S.A. A.S.A is an investigator
488 of the Howard Hughes Medical Institute and the Stowers Institute for Medical Research.
489

490 **Author Contributions**

491 The project was conceived and designed by L.G. and A.S.A. Ultrastructural sample
492 preparation and data collection were by F.G., L.G., K.Y. and M.M. Gene cloning, RNAi
493 and phenotyping were by S.Z. and L.G. Figures were developed by L.G. Data interpretation
494 and manuscript preparation were by L.G. and A.S.A.

495

496 **Figure Legends**

497 **Figure 1 Ultrastructural studies of oocytes at prophase I in *S. mediterranea*.** (A) A
498 section of the planarian ovary. Oocytes were pseudo-colored in light yellow. (B) Type I
499 (pseudo-colored in light green) and Type II (pseudo-colored in light yellow) cells.
500 Arrow=undulation; arrowhead=SYCP. (C) Type III cells (pseudo-colored in light
501 yellow). Arrowhead=vesicles. (D) Type IV cells (pseudo-colored in light yellow).
502 Arrowhead=vesicles. (E) Type V cells (pseudo-colored in light yellow).
503 Arrowhead=vesicles. (F) Free ribosome densities in the cytoplasm (number of free
504 ribosomes per 400nm by 400nm area). Three oocytes were quantified for Type I to Type
505 IV cells. Four oocytes were quantified for Type V cells. For every oocyte, three distant
506 areas were quantified. (G) Distances between distal end of the vesicles to the nuclear
507 envelope. Six oocytes for Type III, four oocytes for Type IV, and three oocytes for Type
508 V cells were quantified. Distance unit is μm . (H) Perinuclear vesicles have double

509 membranes. NE=nuclear envelope. M=mitochondria. R=ribosome. G=Golgi. RER=rough
510 ER. S=perinuclear vesicles. (I) Ribosomes decorate the outer membrane of perinuclear
511 vesicles. S=perinuclear vesicles. R=ribosomes. (J) Perinuclear vesicles can directly
512 connect with nuclear envelope. NPC=nuclear pore complex. S=perinuclear vesicles.
513 NE=nuclear envelope. (K) Perinuclear vesicles are dumpy and close to nuclear envelope
514 in Type III cells. (L) Perinuclear vesicles are in dumbbell shapes in Type V cells.
515 D=dumbbell.

516

517 **Figure 2 3D reconstruction of the Sunburst Nuclear Envelope Vesicles.** (A) Type III
518 cells. Green sheet=NE. Dots=NPC. Purple and red buds=SNEVs. (B) Type IV cells.
519 Cyan sheet=NE. Dots=NPC. Green, Red, Blue, Purple coral shapes=SNEVs. (C) Type V
520 cells. Green sheet=NE. Dots=NPC. The rest=SNEVs. (D-E) The same SNEV sectioned at
521 different positions. N=nucleoplasm. C=cytoplasm. Ribosomes on NE (green sheet) were
522 present but not illustrated. (F-G) The same SNEV viewed from different angles.
523 N=nucleoplasm. C=cytoplasm. Dumbbell shapes in F. (H-I) The same SNEV sectioned at
524 different positions. N=nucleoplasm. C=cytoplasm. Dumbbell shapes in H. Double rings
525 in I.

526

527 **Figure 3 Ultrastructural view of ovulated unfertilized oocytes at metaphase II.** (A)
528 Overview of an unfertilized oocyte at metaphase II. (B) SNEV units in the cytoplasm
529 with various sizes and shapes. (C) From dumpy SNEVs in Type III cells (left), to SNEVs
530 in Type V cells (right), the inner membranes tend to adhere to form NE doublets. Scale
531 bar=1 μ m. (D) SNEV units in metaphase II oocytes have complex organizations, and
532 prominent NE doublets. Dashed line rectangles=NE doublets. C=cytoplasm.
533 N=nucleoplasm. M=mitochondria.

534

535 **Figure 4 Nuclear contents (e.g. proteins) packaged and transported by SNEVs into**
536 **cytoplasm.** Planarian oocytes stained with SMEDWI-2 antibody. Left
537 column=chromosomes with Hoechst 33342 staining. Middle column=SMEDWI-2
538 antibody. Right column=merge. (A) Type III cells. (B) Type IV cells. (C) Type V cells.
539 (D) Rare metaphase II cells in the ovary.

540

541 **Figure 5 Interactions between SNEVs and peripheral ER, and microtubules.** (A-C)
542 Double staining with anti-SEC61A (magenta) and anti-Histone H3 (green) in Type III
543 oocytes (A), and Type V oocytes (B and C). (C) Line profiling to examine co-
544 localizations between peripheral ER (SEC61A, magenta), and SNEVs (Histone H3,
545 green). (D-E) TEM view of peripheral smooth ER (SER) and SNEVs. (F-G) TEM view
546 of microtubules (MT) and SNEVs.

547

548 **Supplementary Figure 1 Characteristic features of a female germ cell.** (A) Overview
549 of a corner of a Type IV oocyte, and five regions which will be zoomed in from a TEM
550 image. N=nuclear. (A1) A.L.=annulate lamellae. L.D.=lipid droplet. (A2) SER=smooth
551 ER. A.L.=annulate lamellae. M=mitochondria. (A3) GI=Cortical granules, type I. (A4)
552 GII=Cortical granules, type II. (A5) M=mitochondria. C=chromatoid body. (B) Summary
553 of the presence and absence of all organelles in different types of cells.

554

555 **Supplementary Figure 2 Type I cells have Synaptonemal Complexes.** (A) TEM
556 images of Type I (middle right) and Type II (top) cells. (B) Synaptonemal Complexes.
557 (C-E) Immuno TEM studies of the Type I cells with anti-ds DNA antibodies. High
558 electron density regions in the Synaptonemal Complexes are dsDNA (E).
559

560 **Supplementary Figure 3 Immunofluorescence staining with SMEDWI-1 and**
561 **Histone H3 antibodies.** (A) A section of a planarian ovary stained with SMEDWI-1
562 antibody. Left=anti-SMEDWI-1. Middle=Hoechst 33342. Right=merge. (B-C) Planarian
563 oocytes stained with Anti-Histone H3 antibody. Anti-Histone H3 (green) in Type III cells
564 (B), and Type V cells (C). DNA is in magenta. Overlap of DNA and Histone H3 is white
565 in color. (D) Schematic illustration of GVBD in mouse and human oocytes (top), nuclear
566 budding/blebbing in somatic cells or oocytes of flies, nematodes, and salamanders
567 (middle), and GVBD to produce SNEVs in the oocytes of *S. mediterranea*.

Figure 1

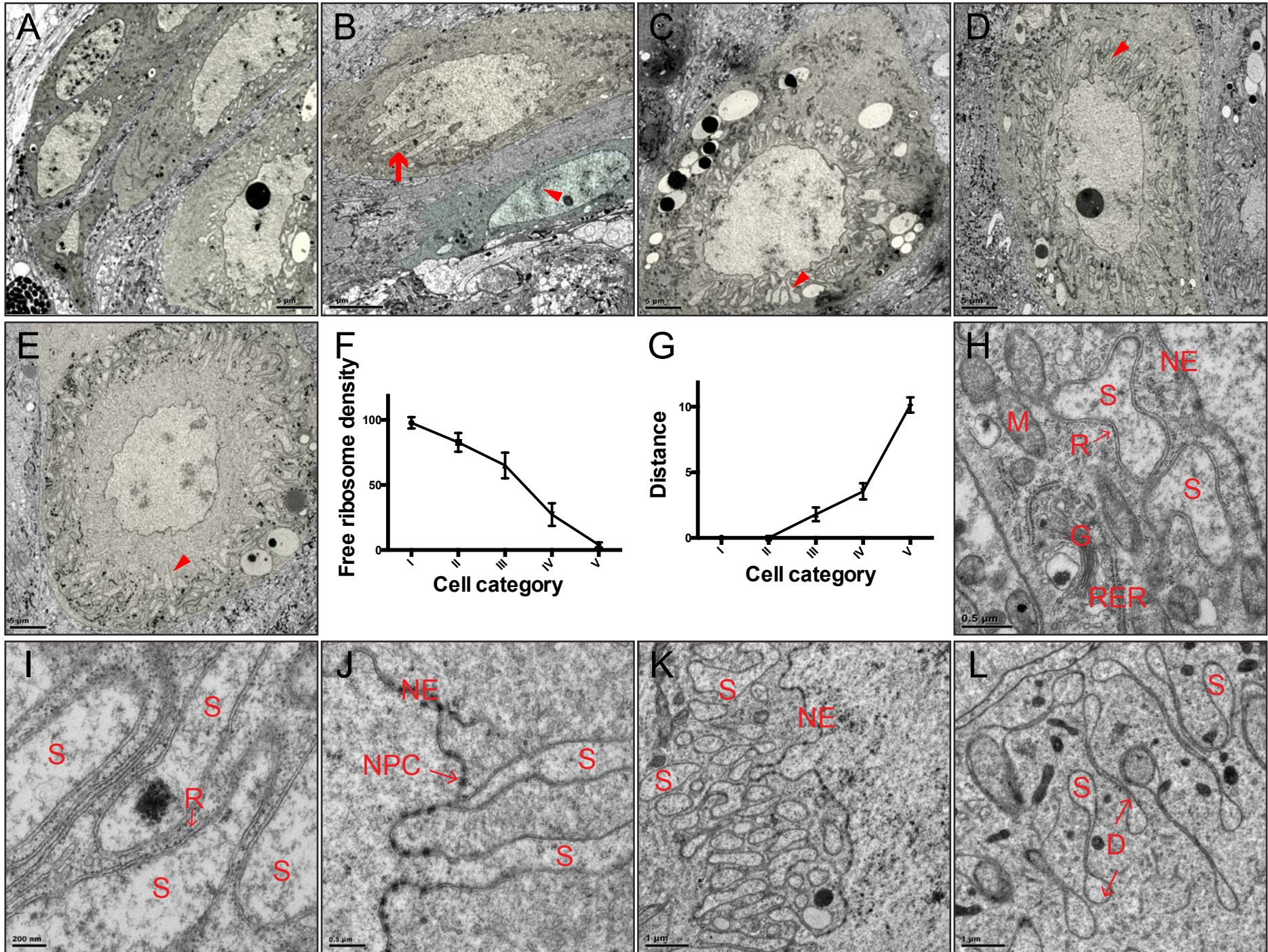


Figure 2

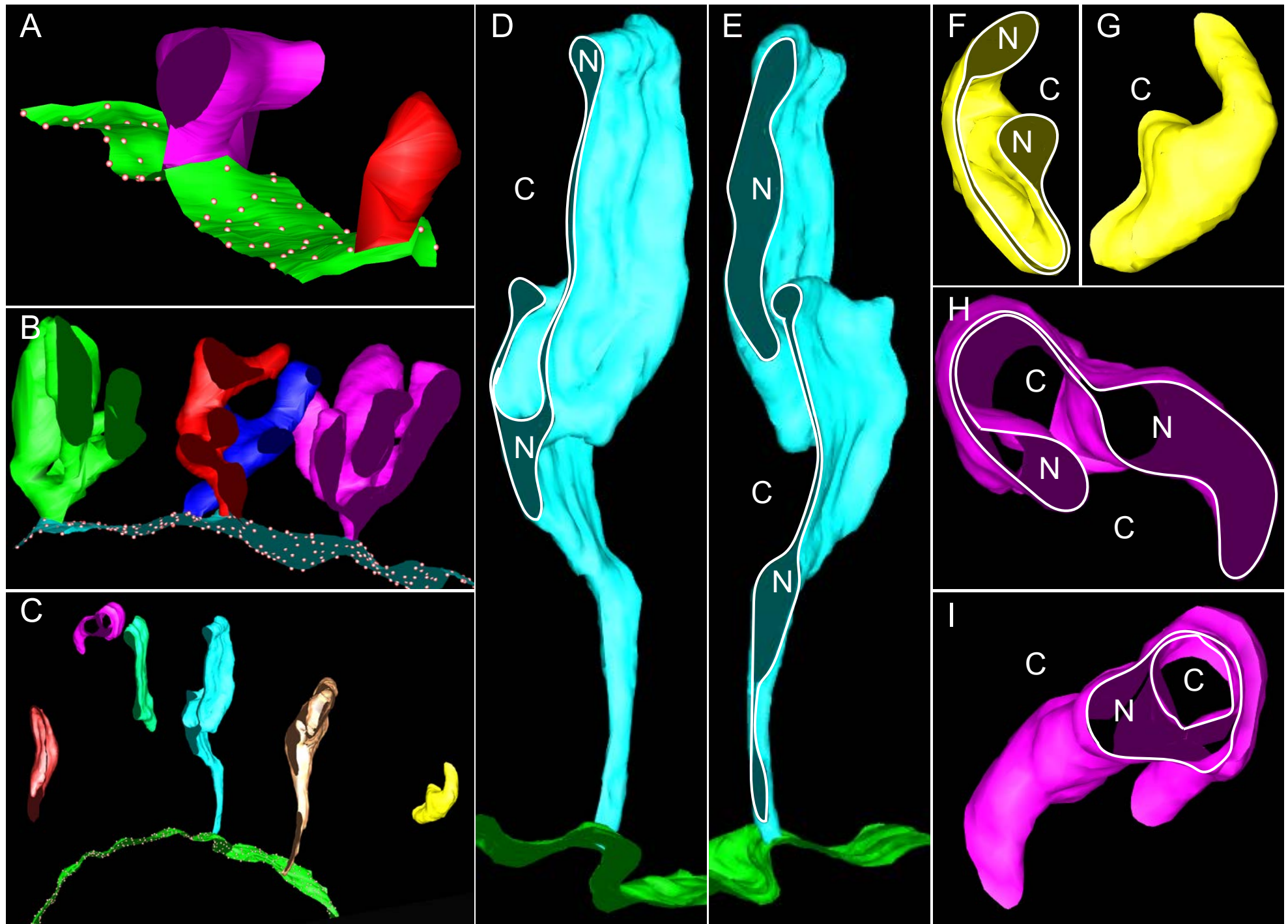
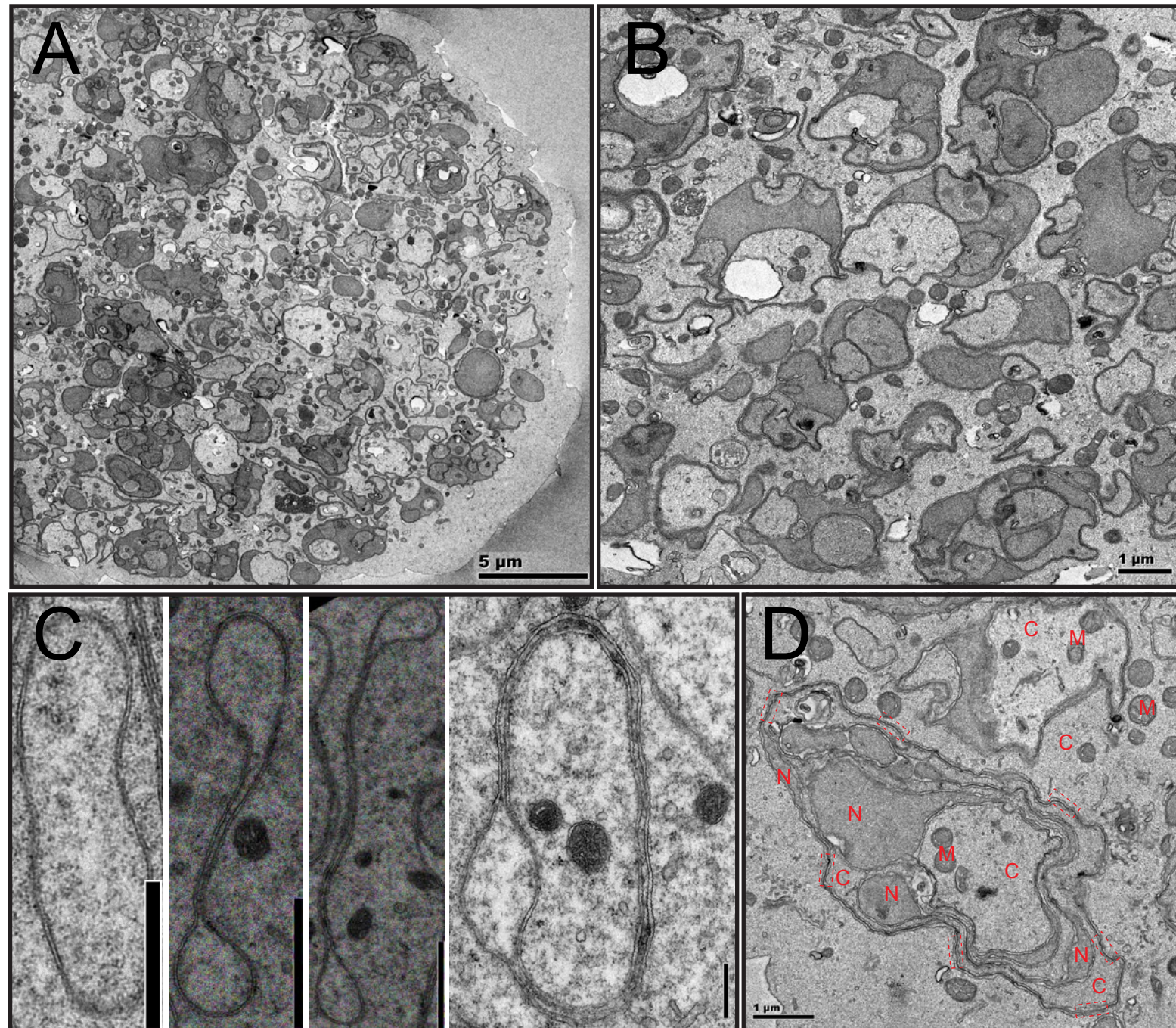


Figure 3



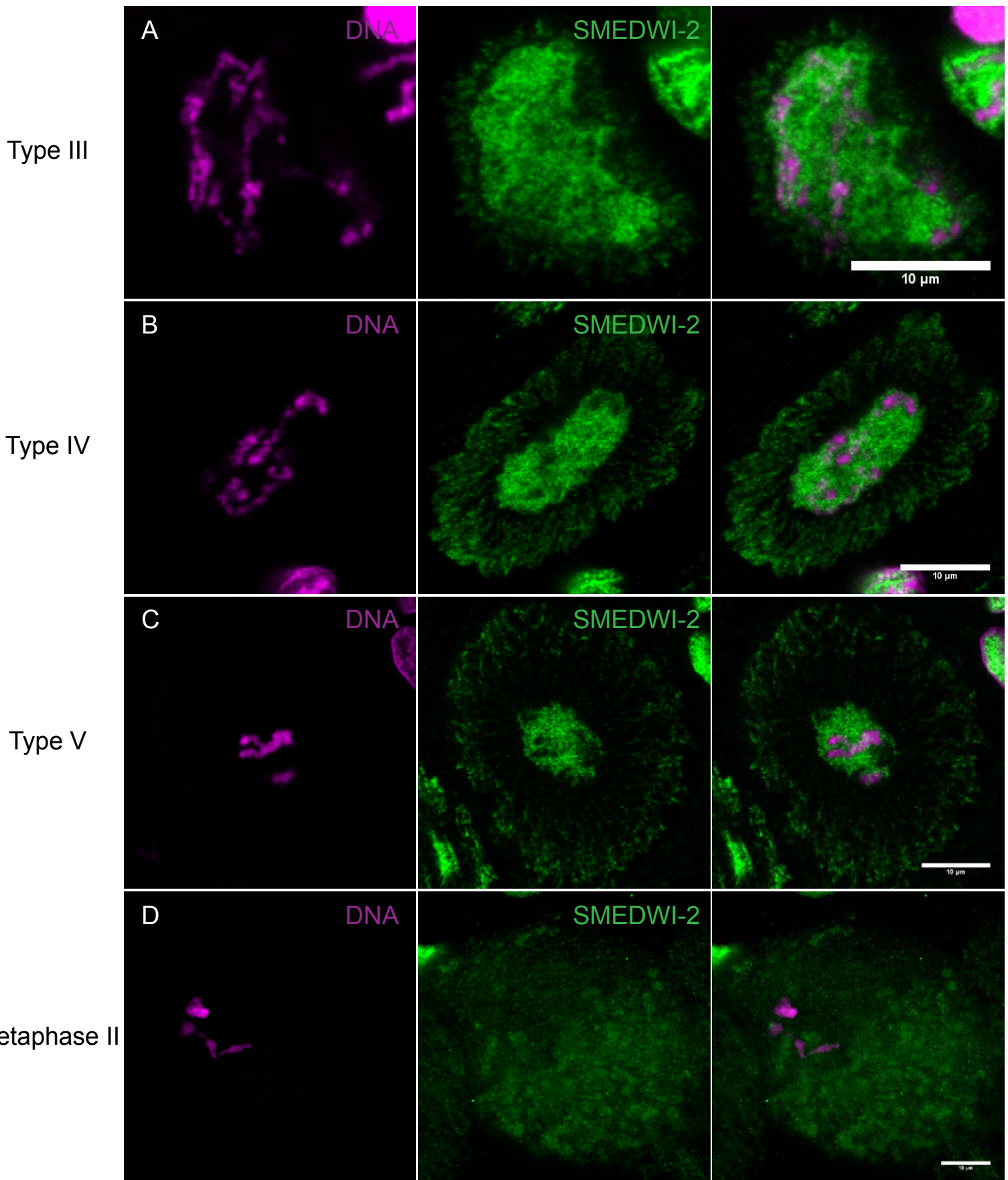
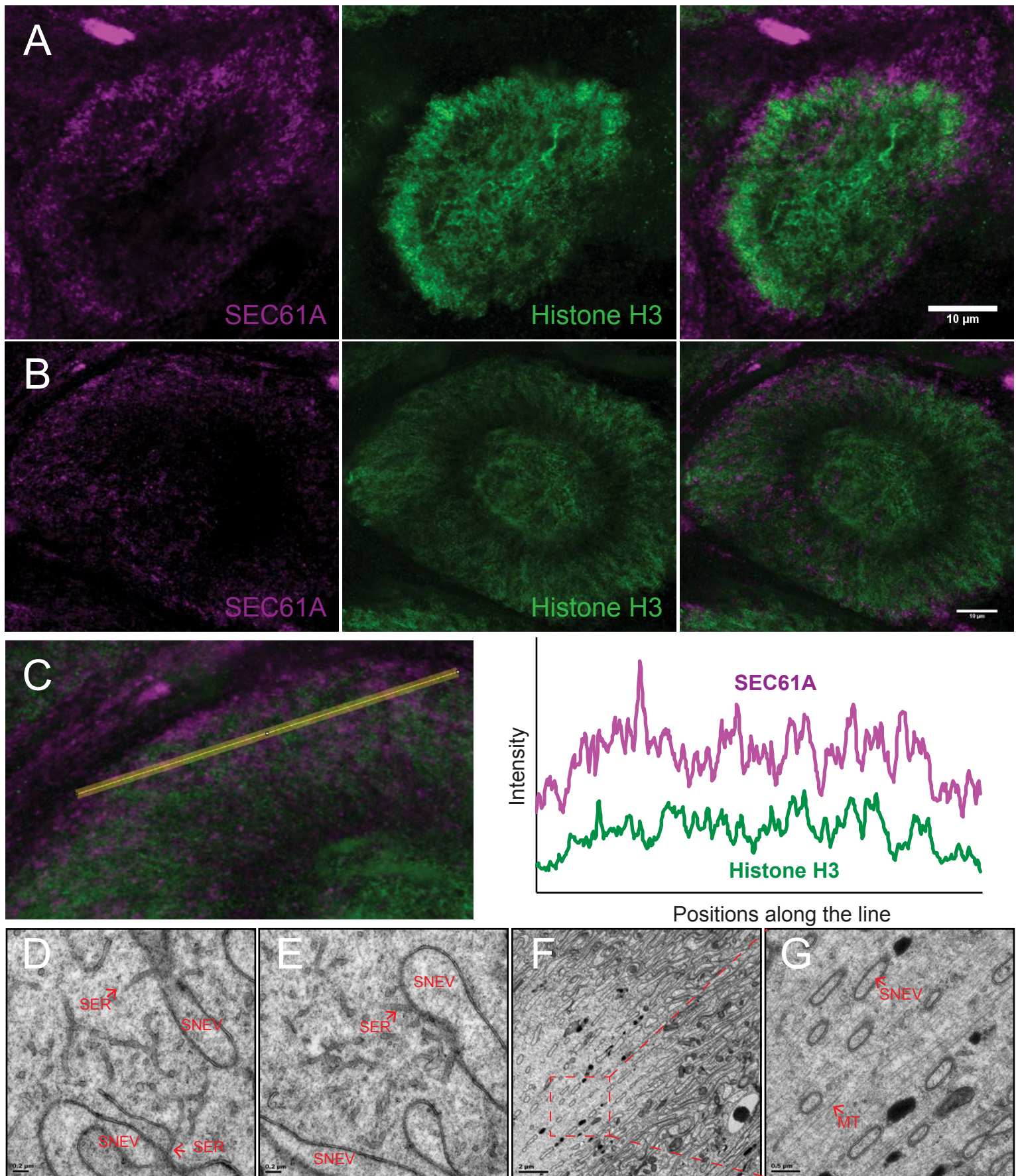
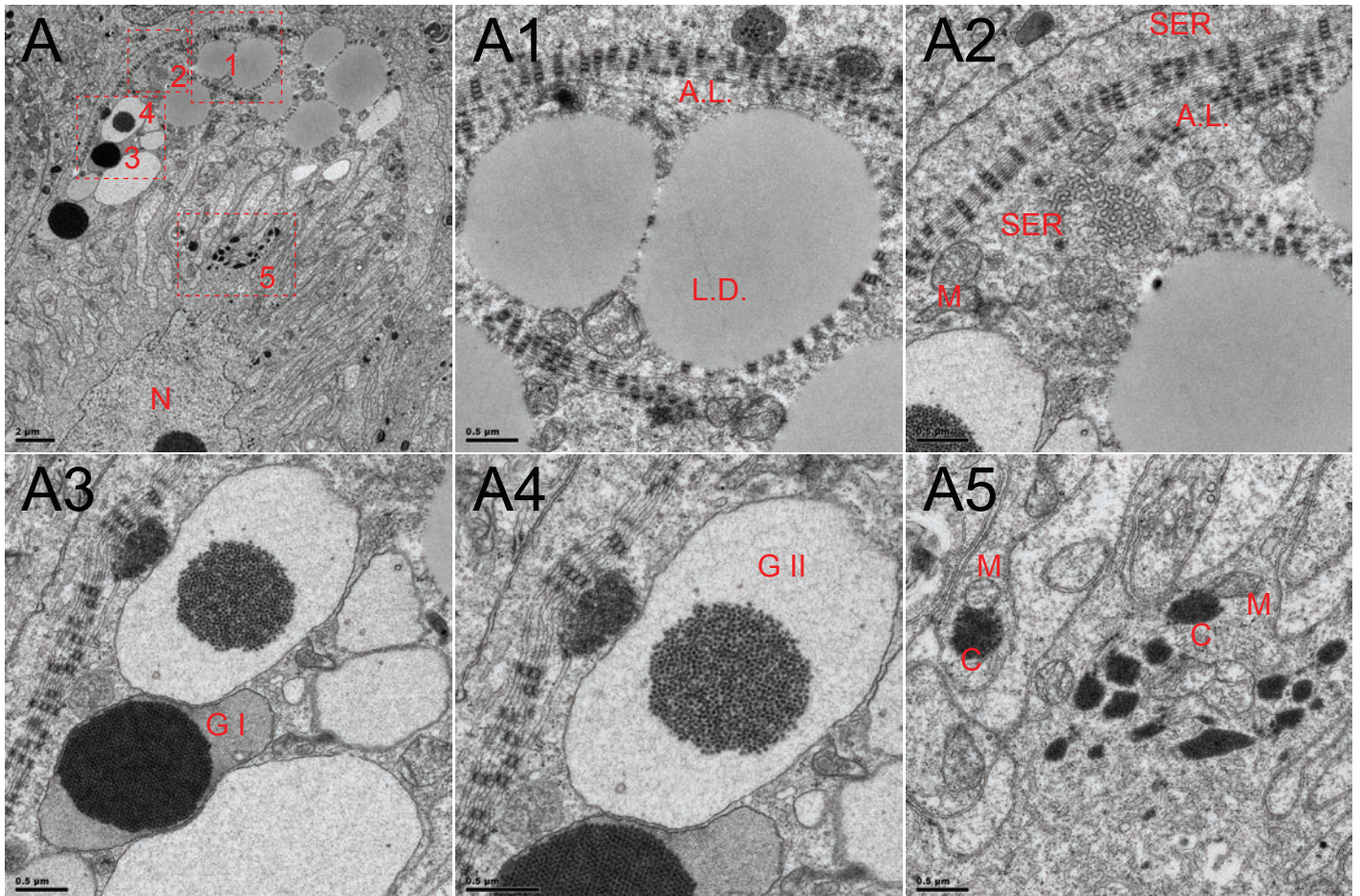


Figure 5

bioRxiv preprint doi: <https://doi.org/10.1101/620609>; this version posted May 5, 2019. The copyright holder for this preprint (which was not certified by peer review) is the author/funder, who has granted bioRxiv a license to display the preprint in perpetuity. It is made available under aCC-BY-NC-ND 4.0 International license.



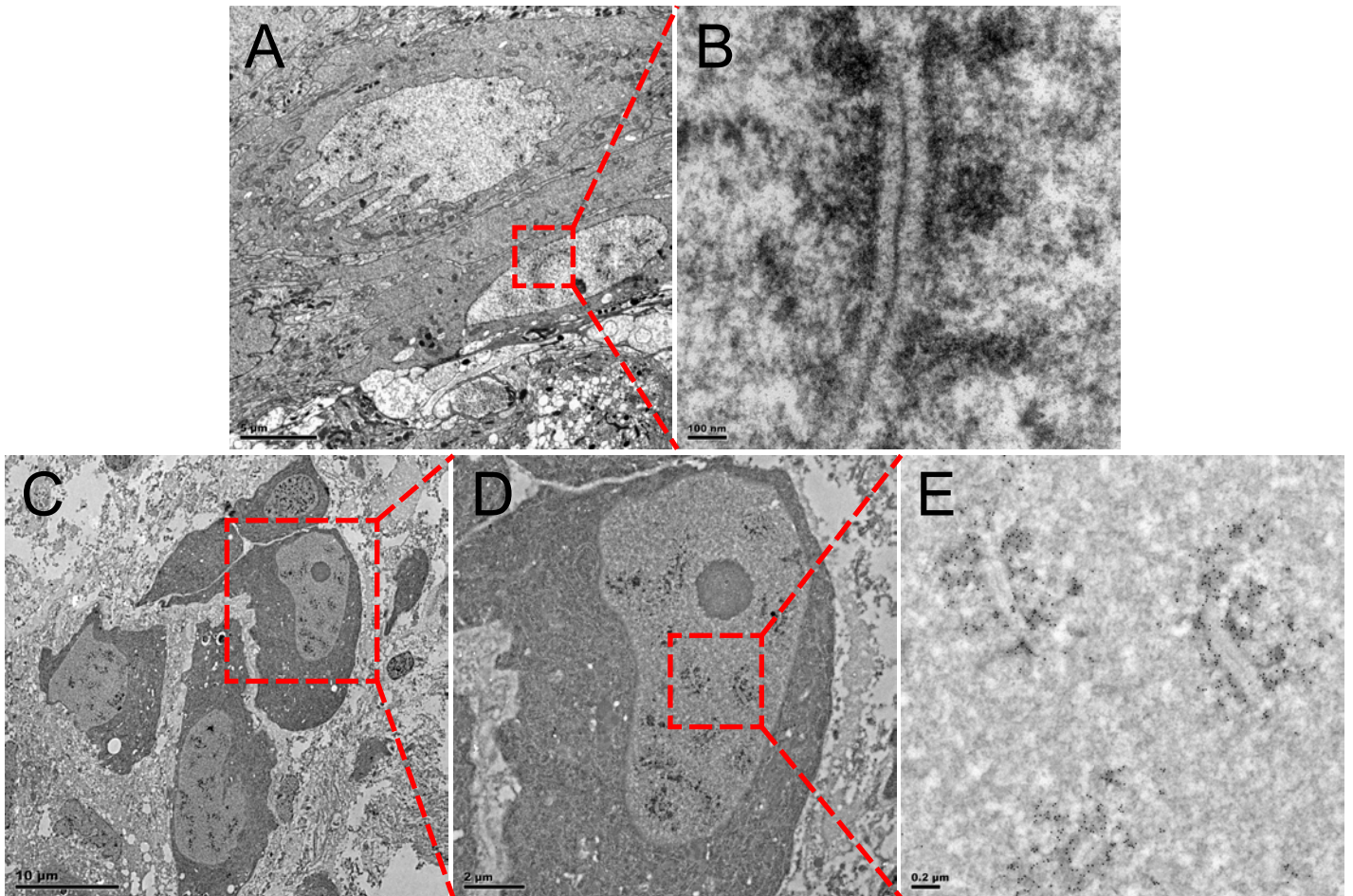
Supplemental Figure 1



B

Features	Categories				
	I	II	III	IV	V
smooth ER	+	+	+	+	+
mitochondria	+	+	+	+	+
Chromatoid Body	+	+	+	+	+
Lipid droplet	+	+	+	+	+
Annulate Lamellae	-	-	+	+	+
Granule I/II	-	-	+	+	+

Supplemental Figure 2



Supplemental Figure 3

